

Published in final edited form as:

*Lab Chip*. 2013 April 21; 13(8): 1586–1592. doi:10.1039/c3lc41366g.

## Spatially monitoring oxygen level in 3D microfabricated cell culture systems using optical oxygen sensing beads

Lin Wang<sup>a</sup>, Miguel A. Acosta<sup>b</sup>, Jennie B. Leach<sup>c</sup>, and Rebecca L. Carrier<sup>d</sup>

<sup>a</sup>Institute for Integrated Cell-Material Sciences (iCeMS), Kyoto University, Yoshida-Ushinomiya-cho, Sakyo-ku, Kyoto, 606-8501, Japan. lwang@icems.kyotou.ac.jp; Fax: +81 75 753-9864; Tel: +81 75 753-9864

<sup>b</sup>UNC/NCSU Joint Department of Biomedical Engineering, 4206D Engineering Building III, 911 Oval Drive, Raleigh, NC 27695, USA. maacost2@ncsu.edu; Fax: +1 919 513 3814; Tel: +1 919 515 5252

<sup>c</sup>UMBC, Department of Chemical, Biochemical & Environmental Engineering, 1000 Hilltop Circle, Baltimore, MD 21250, USA. jleach@umbc.edu; Fax: +1 410 455 1049; Tel: +1 410 455 8152

<sup>d</sup>Northeastern University, Department of Chemical Engineering, 360 Huntington Ave, Boston, MA 02115, USA. rebecca@coe.neu.edu; Fax: +1 617 373 2209; Tel: +1 617 373 7126

### Abstract

Capability of measuring and monitoring local oxygen concentration at the single cell level (tens of microns scale) is often desirable but difficult to achieve in cell culture. In this study, biocompatible oxygen sensing beads were prepared and tested for their potential for real-time monitoring and mapping of local oxygen concentration in 3D micro-patterned cell culture systems. Each oxygen sensing bead is composed of a silica core loaded with both an oxygen sensitive Ru(Ph<sub>2</sub>phen<sub>3</sub>)Cl<sub>2</sub> dye and oxygen insensitive Nile blue reference dye, and a poly-dimethylsiloxane (PDMS) shell rendering biocompatibility. Human intestinal epithelial Caco-2 cells were cultivated on a series of PDMS and type I collagen based substrates patterned with micro-well arrays for 3 or 7 days, and then brought into contact with oxygen sensing beads. Using an image analysis algorithm to convert fluorescence intensity of beads to partial oxygen pressure in the culture system, tens of microns-size oxygen sensing beads enabled the spatial measurement of local oxygen concentration in the microfabricated system. Results generally indicated lower oxygen level inside wells than on top of wells, and local oxygen level dependence on structural features of cell culture surfaces. Interestingly, chemical composition of cell culture substrates also appeared to affect oxygen level, with type-I collagen based cell culture systems having lower oxygen concentration compared to PDMS based cell culture systems. In general, results suggest that oxygen sensing beads can be utilized to achieve real-time and local monitoring of micro-environment oxygen level in 3D microfabricated cell culture systems.

### Introduction

Oxygen plays an important role in cellular function and behavior. Cell growth rate and metabolism, and protein synthesis are strongly dependent on oxygen level in culture medium. Hypoxia/re-oxygenation was found to affect the permeability of intestinal epithelial cell layers,<sup>1</sup> induce stem cell like phenotype in prostate cancer cells,<sup>2</sup> and enhance the proliferation, invasiveness and metastatic potential of tumor cells.<sup>3,4</sup> Hyperoxia leads to reactive oxygen species formation and eventually causes cell injury, inflammatory response, and death in pulmonary cells.<sup>5,6</sup>

The direct and non-invasive measurement of oxygen level in cell culture offers advantages of allowing real time monitoring and adjustment; local measurement and mapping of oxygen level in a 3D cell culture microenvironment would also enable better understanding of the impact of 3D features on oxygen distribution within cell culture systems and related influence on cellular behavior. Previously, we have demonstrated that small intestinal epithelial culture on 3D microfabricated substrates with biomimetic intestinal crypt-like topography (micro-wells with hundred micron scale size) induced small intestinal Caco-2 cells expressing a less differentiated phenotype;<sup>7,8</sup> this finding was particularly interesting in light of the presence of intestinal stem cells in crypts *in vivo*. However, the underlying mechanism of intestinal crypt-like topography in regulating intestinal cell behavior is still not clear.

Hypoxia is known to be an important regulator of stem cell differentiation.<sup>9,10</sup> Hypoxic conditions helps stem cells maintain their undifferentiated phenotype in a reversible fashion.<sup>11–13</sup> When transferred to normoxia conditions, the hypoxic stem cells are able to differentiate.<sup>9</sup> In our system, cells cultured in micro-wells may have diffusion-limited oxygen and nutrient transport, leading to depleted levels at well bottoms relative to tops. Such a locally hypoxic environment (inside micro-well) might be one of the important reasons for a less differentiated cell phenotype of intestinal Caco-2 cells grown on 3D surfaces. To test this hypothesis, we investigate the feasibility of utilizing in-house fabricated biocompatible non-invasive optical oxygen sensing beads for mapping oxygen concentration distribution within 3D intestinal epithelial cell culture systems.

Our oxygen sensing bead operates on the principle of reversible luminescence quenching of Ru(Ph<sub>2</sub>phen<sub>3</sub>)Cl<sub>2</sub> by oxygen. The beads are tens of microns in size and contain a core of silica loaded with both the oxygen-sensitive Ru(Ph<sub>2</sub>phen<sub>3</sub>)Cl<sub>2</sub> dye and an oxygen-insensitive Nile Blue dye (reference dye). The bead shell consists of biocompatible and oxygen permeable polydimethylsiloxane (PDMS) (Fig. 1). Electrode and fluorescence-based sensors are two of the most widely used types of oxygen sensors in literature. Clark type electrode sensors suffer from difficulties in adaptation to continuous and non-invasive monitoring, which makes them not suitable for temporal and spatial monitoring of oxygen level in microfabricated cell culture systems.<sup>14</sup> Optical oxygen sensors based on quenching of fluorescence by oxygen are minimally perturbing, do not consume oxygen, and are adaptable to small volumes, which makes them a preferable system in mapping and monitoring of oxygen level in 3D cell culture systems and living cell-containing microfluidic systems. Compared with other optical sensing systems,<sup>15–18</sup> our system has advantages including: 1) immobilization of oxygen sensitive dye on micron-scale silica bead prevents endocytosis of oxygen sensitive dye and potential cytotoxic effects to living cells; 2) PDMS coating further protects cells from directly contacting oxygen sensing dye, enhances stability of oxygen sensing dye on surface of silica beads, and prevent possible leaking of dye into cell culture medium; 3) the beads' tens of microns scale size facilitates removal and recycling of beads from the cell culture system, meanwhile still allowing single cell level measurement; 4) oxygen levels are determined by measuring the ratio between the emission intensities of the Ru(Ph<sub>2</sub>phen<sub>3</sub>)Cl<sub>2</sub> and Nile Blue reference dyes, removing potential artefacts introduced by uneven dye distribution among different beads; 5) Nile Blue's emission spectrum differs from Ru(Ph<sub>2</sub>phen<sub>3</sub>)Cl<sub>2</sub>'s emission spectrum, which allows independent measurement of their fluorescence; 6) beads offer ease in application and data collection and analysis.

Previously, we have demonstrated the fabrication and characterization of oxygen-sensing beads,<sup>19</sup> and their application in monitoring oxygen transport across bacterial bio-films.<sup>20</sup> Herein, we report the use of our oxygen-sensing beads in measuring oxygen profiles on the contoured surface of a mammalian cell layer on a 3D substrate. The culture substrates

utilized were patterned with micro-well arrays with diameters and depths in the hundreds of microns range, mimicking the surface features of native small intestinal crypts. In order to enable analysis of oxygen levels on microscale features of our system, specifically bottoms and tops of micro-wells, we modified the data analysis protocol to enable analysis of specific beads in specific locations (*i.e.* within or on top of cells), which allows us to measure oxygen level in area with size as small as  $\sim 0.01 \text{ mm}^2$ . The ability of micro-beads to sense and quantitate this micro-environmental oxygen level variation was demonstrated.

## Experimental

### Fabrication of oxygen sensing microbeads

The fabrication of PDMS encapsulated silica particle-based oxygen sensing beads follows a two-step procedure reported by Acosta *et al.*<sup>19</sup> First, the oxygen sensitive luminophore  $\text{Ru}(\text{Ph}_2\text{phen}_3)\text{Cl}_2$  (Ruth) and oxygen insensitive reference fluorophore Nile blue chloride (Nb) were immobilized on the surface of silica beads. Briefly, 10 ml of 0.5 mM  $\text{Ru}(\text{Ph}_2\text{phen}_3)\text{Cl}_2$  and 10 ml 0.5 mM Nile blue chloride in ethanol solution were simultaneously added to 2 g silica gel in 40 ml of 0.01 N NaOH suspension and reacted for 30 min. The dye loaded silica particles were collected through centrifugation and dried at 70 °C overnight. Second, the dye loaded silica beads were further encapsulated in PDMS. 0.2 g of dried silica beads were suspended in 700  $\mu\text{l}$  hexane, 1g of PDMS pre-polymer and 0.1 g curing agent. The above silica bead suspension was then poured into 300 ml 70 °C 2% w/v sodium dodecyl sulfate (SDS) in water solution and stirred at 1200 rpm for 7–8 h. The resulting PDMS encapsulated silica beads were passed through a 0.5 mm sieve and collected by a 25  $\mu\text{m}$  sieve. Beads were then washed three times in 0.2% w/v bovine serum albumin (BSA) in phosphate-buffered saline (PBS) containing 0.1% methyl-4-hydroxybenzoate (methylparaben) and finally suspended in 0.2% BSA in PBS solution at a concentration of  $\sim 50$  particles/ $\mu\text{l}$ .

### Calibration of oxygen sensing beads

The calibration of PDMS encapsulated oxygen sensing bead fluorescence to dissolved oxygen was conducted by embedding beads into a thin layer ( $\sim 250 \mu\text{m}$  in thickness) of poly (ethylene glycol) dimethacrylate (PEG-DM) and loading to a parallel-plate flow chamber with 1 mm thick flow chamber. Water with different dissolved oxygen ( $p\text{O}_2$  from 0 to 135 mmHg) was passed through the chamber, and the fluorescent images of embedded oxygen sensing beads were recorded and processed using image J. For a particular oxygen concentration, an image of Nile blue (Ex/Em = 636/656 nm) and an image of  $\text{Ru}(\text{Ph}_2\text{phen}_3)\text{Cl}_2$  (Ex/Em = 470/610 nm) were recorded. Each fluorescing bead in the Nile blue image was selected, and an average fluorescence intensity of selected beads was acquired. The same selection was made in the corresponding  $\text{Ru}(\text{Ph}_2\text{phen}_3)\text{Cl}_2$  image, and an average fluorescence intensity was also acquired. A two-site Stern–Volmer model was used to correlate fluorescence intensities to dissolved oxygen content:

$$\frac{I_{R,0} - I_R}{I_{R,0} (f_1 - 1) + I_R} = K_{SV} [\text{O}_2] \quad (1)$$

where  $f_1$  ( $f_1 = 0.9$ ) is fraction of quenched population,  $K_{SV}$  is quenching constant,  $I_R$  is the ratio of the fluorescence intensity of  $\text{Ru}(\text{Ph}_2\text{phen}_3)\text{Cl}_2$  and Nile blue chloride,  $I_{R,0}$  is the ratio of two fluorophores when oxygen concentration is zero.  $I_{R,0}$  is obtained from the

regression of  $I_R$  versus  $p\text{O}_2$ , where  $K_{SV}$  is obtained from the regression of  $\frac{I_{R,0} - I_R}{I_{R,0} (f_1 - 1) + I_R}$  versus  $p\text{O}_2$ .

It is noted that there is a certain level of heterogeneity in fluorescent dye distribution among our oxygen sensing beads. For example, some beads do not have a fluorescent dye loaded silica core, resulting in no fluorescence signal, and some beads only have Ruth dye signal without corresponding reference dye signal. To correct the potential error such heterogeneity might bring into final results, beads that do not fluoresce and beads without reference dye are excluded during data processing.

### Monitor local oxygen level in 3D microfabricated cell culture systems

Two micro-fabricated intestinal cell culture systems were used in this study: PDMS-based<sup>8</sup> and type I collagen-based,<sup>7</sup> each containing micro-wells with diameters and depths in the hundreds of microns range. Caco-2, a human colon carcinoma cell line, was cultivated on the surfaces of patterned substrates for 3 or 7 days and then incubated with ~1350 oxygen sensitive particles/cm<sup>2</sup> of culture surface for either 1 h or 24 h. Ru(Ph<sub>2</sub>phen<sub>3</sub>)Cl<sub>2</sub> and Nile blue fluorescence images focusing on the top and bottom surfaces of micro-wells were recorded. Soft-lithography technique was utilized to fabricate a PDMS substrate patterned with micro-well array (50, 100, or 500  $\mu$ m in diameter, 50  $\mu$ m in spacing, and 120  $\mu$ m in depth) as previously described.<sup>8</sup> Patterned PDMS substrates were affixed to well bottoms of a 12 well cell culture plate using pre-curing PDMS, incubated with 50  $\mu$ g ml<sup>-1</sup> fibronectin (Fn) for 2 h, and then washed three times with PBS. Patterned collagen membranes were fabricated as previously described.<sup>7</sup> Briefly, 5 ml of 5 mg ml<sup>-1</sup> type I collagen from bovine Achilles tendon in 0.05 M acetic acid was dispersed on top of a 3.5 cm<sup>2</sup> PDMS slab patterned with microwell arrays (100 or 500  $\mu$ m in diameter, 50  $\mu$ m in spacing, and 120  $\mu$ m in depth), degassed for 30 min and air-dried overnight. The dried patterned collagen membrane was lifted off from the PDMS mold and baked in an oven at 105 °C overnight to thermally crosslink the collagen. The crosslinked membrane was then affixed to the bottom of a circular cell culture insert and rehydrated overnight in PBS, followed by exhaustive washing with PBS. Before cell culture, inserts were transferred to 12 well plates, and the top surfaces of patterned membranes were incubated with 10  $\mu$ g ml<sup>-1</sup> laminin (Ln) from Engelbreth-Holm-Swarm murine sarcoma for 2 h, and then washed three times with PBS.

Caco-2 cells were seeded onto tops of test surfaces at a density of  $2 \times 10^4$  cells cm<sup>-2</sup>, and cultivated in Eagle's minimum essential medium supplemented with 20% fetal bovine serum (FBS) and 1% antibiotic antimycotic solution at 37 °C 5% CO<sub>2</sub>. Medium was changed every 2 days in culture.

### Statistical analysis

A two-sample *t*-test assuming unequal variance was used as a statistical test. Results are expressed as means  $\pm$  standard error (SE), and were considered significant at  $P < 0.05$  (\*) and  $P < 0.1$  (#).

### Results and discussion

Tens of microns size biocompatible oxygen sensing beads loaded with oxygen-sensitive Ru(Ph<sub>2</sub>phen<sub>3</sub>)Cl<sub>2</sub> dye can enable local, real-time, and dynamic monitoring of oxygen levels in cell culture systems. Utilizing these beads, the measurement of oxygen level requires only a fluorescence microscope, which is generally readily available in biology labs. These properties make our oxygen sensing beads a preferable mode of monitoring and mapping oxygen concentration within a 3D microfabricated cell culture system or a microfluidic system. In this study, Ru(Ph<sub>2</sub>phen<sub>3</sub>)Cl<sub>2</sub> loaded PDMS encapsulated oxygen sensing beads were utilized to monitor the oxygen concentration of intestinal epithelial Caco-2 cultures grown on surfaces of micro-well patterned PDMS and collagen substrates (Fig. 1) to demonstrate the potential usage of these beads for monitoring oxygen level in 3D

microfabricated cell culture systems. A set of flat and patterned (50  $\mu\text{m}$ , 100  $\mu\text{m}$ , and 500  $\mu\text{m}$  wide and 120  $\mu\text{m}$  deep micro-wells) PDMS substrates, and a set of flat and patterned (70  $\mu\text{m}$  wide and 80 mm deep or 500  $\mu\text{m}$  wide and 140  $\mu\text{m}$  deep micro-wells) type I collagen membranes, were used to cultivate intestinal epithelial Caco-2 cells for 3 days or 7 days and then used for testing oxygen sensing beads. Beads were incubated with cells for either 1 h or 24 h, and beads incubated with flat or patterned PDMS or collagen surfaces without cells were used as controls.

### Oxygen sensing beads calibration

The calibration of oxygen sensing beads response to ranges of 0–135 mmHg of oxygen ( $p\text{O}_2$ ) was performed in a flow chamber. Fluorescence intensity of oxygen sensing beads was calculated and fit to a two-site Stern–Volmer model.  $I_{R,0}$  is obtained from the regression

of  $I_R$  versus  $p\text{O}_2$ , where  $K_{SV}$  is obtained from the regression of  $\frac{I_{R,0} - I_R}{I_{R,0}(f_1 - 1) + I_R}$  versus  $p\text{O}_2$ . The results of regression show that  $I_{R,0} = 9.5$  and  $R^2 = 0.924$  (Fig. 2A), and the Stern–Volmer quenching constant  $K_{SV} = 0.0218 \text{ mmHg}^{-1}$  and  $R^2 = 0.898$  (Fig. 2B). The  $I_{R,0}$  and  $K_{SV}$  values were then used for the calculation of  $p\text{O}_2$  in the following studies. Substitute  $I_{R,0}$

and  $K_{SV}$ , the two-site Stern–Volmer equation is written as  $\frac{9.5 - I_R}{9.5(-0.1) + I_R} = 0.0218 p\text{O}_2$ , where

$I_R = \frac{R_{\text{uth}}}{N_b}$ . Using the calibrated two-site Stern–Volmer model, oxygen partial pressure with values of 0 to 10 mm Hg can be calculated with approximately 25% error, while oxygen partial pressures of 10 to 25 mm Hg and 25 mm Hg and above have approximately 17% and 6% error, respectively.<sup>19</sup>

### Caco-2 cell growth on microfabricated PDMS and collagen-based systems

The cytoskeleton F-actin staining and cell nuclei DAPI staining of Caco-2 cells cultivated on PDMS and collagen substrates patterned with 500  $\mu\text{m}$  micro-wells for 3 and 7 days (Fig. 3) suggest that with initial seeding density  $2 \times 10^4 \text{ cells cm}^{-2}$  on both patterned PDMS and collagen substrates, cell density increased from day 3 to day 7. By day 7, collagen surfaces are fully covered by cells, and more than 90% of PDMS surfaces are covered by cells. Caco-2 cells spread faster on PDMS surfaces than on collagen surfaces, as evidenced by almost 70–80% cell coverage on PDMS substrates and 50–60% cell coverage on collagen substrates at day 3. It was also noted that cells grew in higher density on collagen substrates, as at day 7 cell nuclei density on collagen surfaces is higher than nuclei density on corresponding PDMS surfaces (Fig. 3).

### Monitoring spatial oxygen level using oxygen sensing beads

Microscopic images of introduction of oxygen sensing beads to Caco-2 cells cultivated on flat and patterned PDMS and collagen surfaces at day 3 and day 7 (Fig. 4 A, B) show that oxygen sensing beads are readily incorporated onto cell culture surfaces and observed by fluorescence microscopy. Beads are distributed throughout patterned surfaces and present at both tops and bottoms of micro-well structures, allowing the local monitoring of oxygen levels of 3D surfaces (*i.e.* top of well and inside of well). In general, the fluorescence intensities of  $\text{Ru}(\text{Ph}_2\text{phen}_3)\text{Cl}_2$  (in red) of beads located inside wells are higher than those of beads located on tops of wells, suggesting the oxygen concentration difference related to surface geometry of cell culture substrates. The fluorescence intensity of  $\text{Ru}(\text{Ph}_2\text{phen}_3)\text{Cl}_2$  beads introduced to day 3 culture is higher than those introduced to day 7 culture, indicating that the oxygen concentration relates inversely with cell density, with higher cell density leading to higher level of oxygen depletion. Fluorescence intensity of  $\text{Ru}(\text{Ph}_2\text{phen}_3)\text{Cl}_2$  beads introduced to PDMS-based substrates is higher than that of beads introduced to



collagen-based substrates, likely due to the higher cell density on collagen surfaces compared to PDMS surfaces or possible higher cellular metabolism rate on collagen surfaces, or both.

Calculated partial oxygen pressure ( $pO_2$ ) distributions on the surfaces of 3D PDMS-based and collagen-based intestinal epithelial Caco-2 culture systems are plotted in Fig. 5. On all surfaces,  $pO_2$  generally decreases with culture time, as expected, since increases in cell growth and density in a closed cell culture system likely result in oxygen depletion. After 7 days of culture, the  $pO_2$  on cell surfaces became less than 20 mmHg (hypoxic condition). In the PDMS-based system (Fig. 5A, B, C, and D), geometry of 3D surfaces seems to affect  $pO_2$  level and distribution, evidenced by different  $pO_2$  readings on cell-free flat and micro-well patterned surfaces. The  $pO_2$  measurement on cell free PDMS substrates falls in the range of normoxic conditions (30–90 mmHg). When cultivated with Caco-2 cells,  $pO_2$  values are generally lower than corresponding cell-free PDMS surfaces. The decrease of  $pO_2$  from 1 h-incubation to 24 h-incubation with oxygen sensing beads in cell containing substrates might be due to continuous growth of cells during the 24 h-incubation period leading to further depletion of oxygen in cell culture medium, or possibly due to transient mixing effects after introduction of beads.

$pO_2$  of cells cultivated on flat substrates (both PDMS and collagen) are lower than  $pO_2$  of cells cultivated on micro-well patterned surfaces. It was previously observed that micro-well structure inhibited Caco-2 cell growth for 1–3 days;<sup>7,8</sup> thus, the low  $pO_2$  on flat surface might relate to higher proliferation rate of cells. In addition, on PDMS substrates patterned with 100  $\mu$ m and 500  $\mu$ m wells (Fig. 5C and D)  $pO_2$  levels inside wells are generally lower than  $pO_2$  levels on tops of wells, suggesting the possible oxygen transport limit inside wells, higher cell density inside wells, or higher metabolic activities of cells located inside wells. The fact that these differences are not noted 24 h after adding the beads, except in the cultures with high cell densities (7 day PDMS and collagen substrates) indicates that mixing upon addition of medium (and beads) may impact oxygen level differences on micro-fabricated substrates. These results suggest that our oxygen sensing beads can be utilized to dynamically monitor oxygen level fluctuations and their micro-scale variation in 3D microfabricated cell culture systems.

Interestingly, in the case of PDMS substrates, the difference of oxygen concentration between top and bottom of the wells is inversely proportional to well size. Substrates patterned with 500  $\mu$ m micro-wells have the largest difference in oxygen concentration from top to bottom of well, while there is no such measurable difference with 50  $\mu$ m micro-wells (Fig. 5B, C, D). This might be due to the fact that PDMS is highly permeable to gas, with diffusivity of oxygen approximately twice as high as diffusivity of oxygen in water.<sup>21</sup> In the case of small wells (*i.e.* 50  $\mu$ m), oxygen concentration in the relatively small volume of water inside wells may be more quickly or easily adjusted by surrounding highly permeable PDMS comparing with 500  $\mu$ m wells, which have 100 times larger volume of water in each well. Previously, it was demonstrated that inhibition of differentiation of Caco-2 cells cultured on micro-well patterned PDMS substrates was most significant for 500  $\mu$ m wells.<sup>8</sup> Oxygen level in cell culture microenvironment has long been known to be one of the important factors in influencing stem cell phenotype. In the small intestine, hypoxia has been related to regulating Notch signaling, which is critical for the maintenance of undifferentiated stem cell populations in the intestinal crypt.<sup>22,23</sup> The distinctive difference of oxygen concentration from top to bottom of 500  $\mu$ m wells may therefore result in a less-differentiated phenotype in Caco-2 cells.

The generally lower  $pO_2$  of cells growing on collagen-based substrates (Fig. 5E, F, and G) compared with PDMS-based substrates might be due to the fact that cells are more densely

packed on the surface of collagen (Fig. 3). On collagen surfaces patterned with 500  $\mu\text{m}$  wells,  $p\text{O}_2$  inside wells is lower than  $p\text{O}_2$  on tops of wells (Fig. 5G). Interestingly, it was found that  $p\text{O}_2$  on the surface of cell-free collagen membrane is extremely low, falling in the range of  $\sim 10$  mmHg (Fig. 5E, F, and G). The depletion of medium oxygen in the vicinity of the collagen membrane may be due to adsorption of oxygen from surrounding medium on the highly porous collagen membrane.

## Conclusions

In conclusion, biocompatible optical oxygen sensing beads tens of microns in size can be used to continuously monitor and map oxygen levels in 3D microfabricated cell culture systems during cell growth, with no medium sampling required. Oxygen sensing beads approximately the same size as single cells allow the local measurement of oxygen level in an area with size  $\sim 0.01$  mm<sup>2</sup>. Real-time monitoring of local oxygen concentration of intestinal epithelial Caco-2 cells cultivated on 3D PDMS and collagen-based surfaces patterned with micro-well arrays utilizing these oxygen sensing beads suggests that 3D geometry of cell culture surfaces affects local oxygen level and its distribution. Oxygen levels inside of micro-wells are generally lower than oxygen levels on top of wells. Depletion of oxygen in culture medium upon culture was also observed, with the level of depletion dependent on type of culture surface (PDMS vs. type I collagen). Our oxygen sensing beads allow the direct integration within cell culture systems, reducing the need for external instruments to acquire data and allowing *in situ* measurement at the time of interest.

## Notes and references

1. Xu D-Z, Lu Q, Kubicka R, Deitch EA. J. Trauma: Inj. Infect. Crit. Care. 1999; 46:280–285.
2. Ma Y, Liang D, Liu J, Axcrone K, Kvalheim G, Stokke T, Nesland JM, Suo Z. PLoS One. 2011; 6:e29170. [PubMed: 22216200]
3. Pennacchietti S, Michieli P, Galluzzo M, Mazzone M, Giordano S, Comoglio PM. Cancer Cell. 2003; 3:347–361. [PubMed: 12726861]
4. Harris AL. Nat. Rev. Cancer. 2002; 2:38–47. [PubMed: 11902584]
5. Crapo JD. Annu. Rev. Physiol. 1986; 48:721–731. [PubMed: 3518622]
6. Mantell LL, Lee PJ. Mol. Genet. Metab. 2000; 71:359–370. [PubMed: 11001828]
7. Wang L, Murthy SK, Barabino GA, Carrier RL. Biomaterials. 2010; 31:7586–7598. [PubMed: 20643478]
8. Wang L, Murthy SK, Fowle WH, Barabino GA, Carrier RL. Biomaterials. 2009; 30:6825–6834. [PubMed: 19766306]
9. Yeung TM, Gandhi SC, Bodmer WF. Proc. Natl. Acad. Sci. U. S. A. 2011
10. Simon MC, Keith B. Nat. Rev. Mol. Cell Biol. 2008; 9:285–296. [PubMed: 18285802]
11. Jögi A, Øra I, Nilsson H, Lindeheim Å, Makino Y, Poellinger L, Axelsson H, Pählman S. Proc. Natl. Acad. Sci. U. S. A. 2002; 99:7021–7026. [PubMed: 12011461]
12. Covello KL, Kehler J, Yu H, Gordan JD, Arsham AM, Hu C-J, Labosky PA, Simon MC, Keith B. Genes Dev. 2006; 20:557–570. [PubMed: 16510872]
13. Gustafsson MV, Zheng X, Pereira T, Gradin K, Jin S, Lundkvist J, Ruas JL, Poellinger L, Lendahl U, Bondesson M. Dev. Cell. 2005; 9:617–628. [PubMed: 16256737]
14. Suzuki H, Hirakawa T, Hoshi T, Toyooka H. Sens. Actuators, B. 2001; 76:565–572.
15. Mehta G, Mehta K, Sud D, Song J, Bersano-Begey T, Futai N, Heo YS, Mycek M-A, Linderman J, Takayama S. Biomed. Microdevices. 2007; 9:123–134. [PubMed: 17160707]
16. Chen W, Lisowski M, Khalil G, Sweet IR, Shen AQ. PLoS One. 2012; 7:e33070. [PubMed: 22479359]
17. Chang-Yen DA, Gale BK. Lab Chip. 2003; 3:297–301. [PubMed: 15007462]

18. John GT, Klimant I, Wittmann C, Heinzle E. *Biotechnol. Bioeng.* 2003; 81:829–836. [PubMed: 12557316]
19. Acosta MA, Ymele-Leki P, Kostov YV, Leach JB. *Biomaterials.* 2009; 30:3068–3074. [PubMed: 19285719]
20. Acosta MA, Velasquez M, Williams K, Ross JM, Leach JB. *Biotechnol. Bioeng.* 2012; 109:2663–2670. [PubMed: 22511120]
21. Charati SG, Stern SA. *Macromolecules.* 1998; 31:5529–5535.
22. Mazumdar J, Dondeti V, Simon MC. *J. Cell. Mol. Med.* 2009; 13:4319–4328. [PubMed: 19900215]
23. Wilson A, Radtke F. *FEBS Lett.* 2006; 580:2860–2868. [PubMed: 16574107]



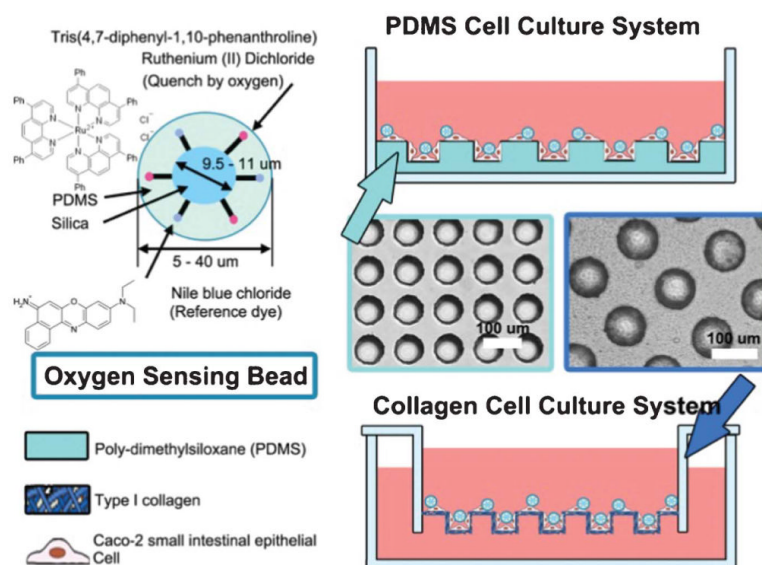


**Fig. 1.** Schematic drawing of the composition and structure of oxygen sensing beads and application of oxygen sensing beads to PDMS and collagen based 3D intestinal epithelial Caco-2 culture system for real time mapping of oxygen level distribution on the culture surface.

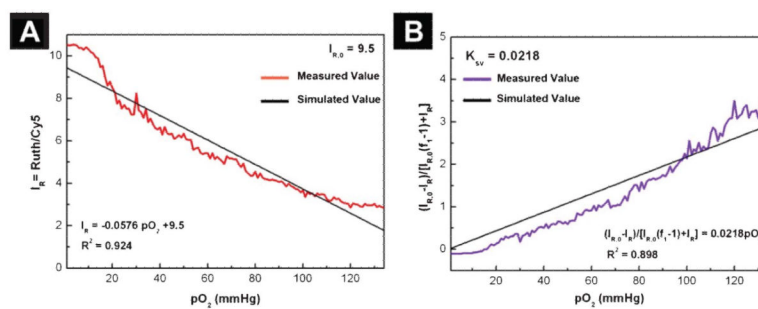


**Fig. 2.** Calibration of oxygen sensing beads using two-site Stern–Volmer model. (A) regression of

$I_R$  versus  $pO_2$  and (B) regression of  $\frac{I_{R,0} - I_R}{I_{R,0}(f_1 - 1) + I_R}$  versus  $pO_2$ .

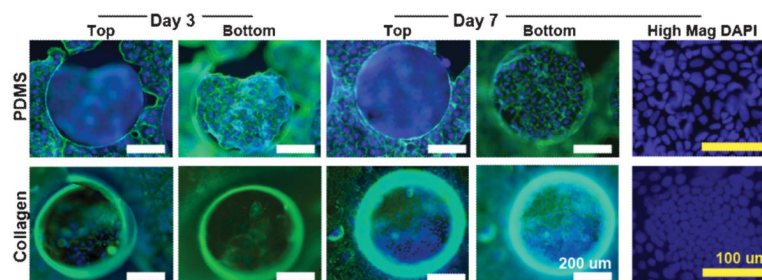


**Fig. 3.**

Coverage of cells on the surface of PDMS and collagen patterned with 500  $\mu\text{m}$  micro-wells after culturing for 3 days and 7 days. Cytoskeleton is stained in green (F-actin staining) and cell nuclei are stained in blue with DAPI. Scale bar: white, 200  $\mu\text{m}$ ; yellow, 100  $\mu\text{m}$ .

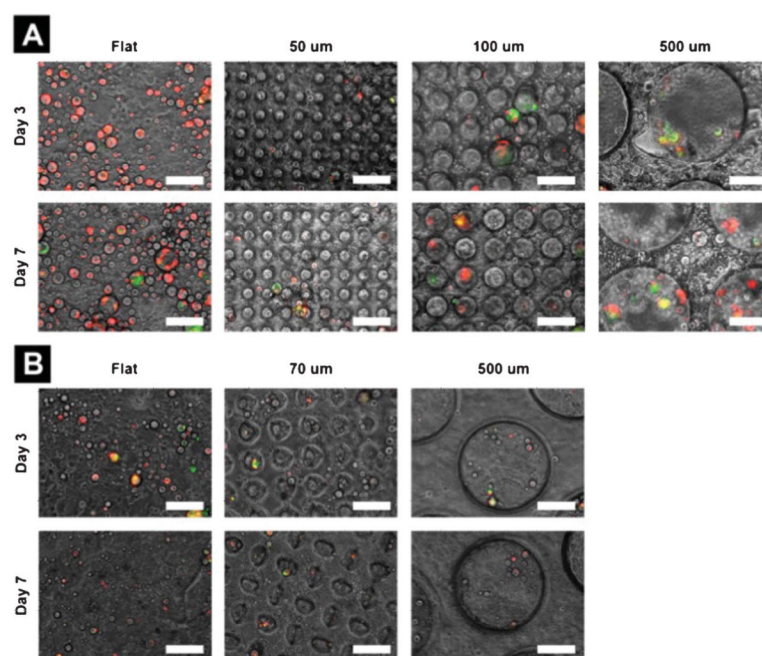


**Fig. 4.** Incubation of oxygen sensing beads with cells cultured on PDMS-based (A) and collagen-based (B) substrates (flat or patterned with micro-wells) for optical and local monitoring of oxygen level in a 3D microfabricated cell culture system. Overlay of fluorescent image of oxygen sensing beads (oxygen sensitive  $\text{Ru}(\text{Ph}_2\text{phen}_3)\text{Cl}_2$  dye is red and oxygen insensitive reference Nile blue dye is green) with phase contrast image of cells cultivated for 3 or 7 days and incubated with oxygen sensing beads for 24 h. Scale bar: 200  $\mu\text{m}$ .

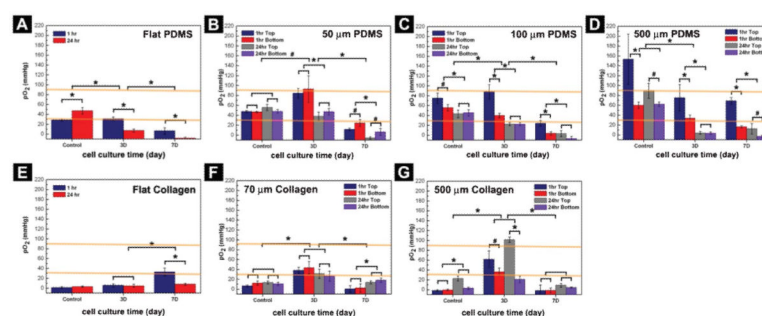


**Fig. 5.**

Calculated partial oxygen pressure ( $pO_2$ ) distributions on the surfaces (tops and bottoms of micro-wells) of 3D PDMS-based (A, B, C, D) and collagen-based (E, F, G) intestinal epithelial Caco-2 culture systems. Caco-2 cells were cultured on 3D PDMS and collagen-based surfaces for 3 days (3D) or 7 days (7D) before incubation with oxygen sensing beads for 1 h or 24 h. Controls are bare 3D PDMS or collagen surfaces without Caco-2 cells. The area between orange lines indicates normoxia (30–90 mmHg).  $P < 0.05$  (\*) and  $P < 0.1$  (#).